Amyotrophic Lateral Sclerosis. 2010; 11: 157–165

informa
healthcare

ORIGINAL ARTICLE

Combined structural and neurochemical evaluation of the corticospinal tract in amyotrophic lateral sclerosis

TIMOTHY PYRA[1], BENJAMIN HUI[2], CHRIS HANSTOCK[4], LUIS CONCHA[4], JOHN C. T. WONG[5], CHRISTIAN BEAULIEU[4], WENDY JOHNSTON[3] & SANJAY KALRA[3,4]

[1]*The Faculty of Medicine and Dentistry,* [3]*Division of Neurology, Department of Medicine,* [4]*Department of Biomedical Engineering, The University of Alberta,* [2]*The Division of Neurology, Department of Medicine, University of Toronto, and* [5]*The Department of Medicine, University of British Columbia*

Abstract

Our objective was to characterize the structural and metabolic changes of the corticospinal tract (CST) in ALS patients using combined diffusion tensor imaging (DTI) and magnetic resonance spectroscopic imaging (MRSI). Fourteen patients (male:female, 6:8; mean age, 54 years) and 14 controls (male:female, 8:6; mean age, 53 years) underwent imaging. Four regions of the CST were evaluated: precentral gyrus, corona radiata, posterior limb of the internal capsule, and cerebral peduncle. DTI and MRSI indices tested included fractional anisotropy (FA), apparent diffusion coefficient (ADC), and the ratio of N-acetylaspartate to choline (NAA/Cho) and creatine (NAA/Cr). In the precentral gyrus, NAA/Cho was reduced 18% ($p < 0.001$), NAA/Cr was reduced 9% ($p = 0.01$), and FA was reduced 3% ($p = 0.02$). NAA/Cho and NAA/Cr were reduced in the corona radiata ($p < 0.001$). Reduced NAA/Cho in the precentral gyrus correlated with shorter symptom duration ($r = 0.66$, $p = 0.02$) and faster disease progression ($r = -0.65$, $p = 0.008$). Increased spasticity correlated with higher ADC in the precentral gyrus ($R = 0.52$, $p = 0.005$). In conclusion, both MRSI and DTI provided in vivo evidence of intracranial degeneration of the CST in ALS that was most prominent rostrally in the precentral gyrus.

Key words: *Diffusion tensor imaging, magnetic resonance spectroscopy, amyotrophic lateral sclerosis, surrogate markers, imaging*

Introduction

Clinical assessment of upper motor neuron (UMN) degeneration in ALS patients is sub-optimal due to the semi-objective nature of the clinical exam and because UMN signs can be attenuated by severe concomitant lower motor neuron (LMN) degeneration. Electrophysiological techniques such as motor unit number estimation can objectively evaluate LMN involvement. However, the inability to quantify UMN disease burden is a serious impediment to understanding pathogenesis and contributes to delays in diagnosis.

Diffusion tensor imaging (DTI) and magnetic resonance spectroscopy (MRS) have emerged as potential surrogates of cerebral degeneration in ALS. DTI can assess the integrity of white matter tracts. This is quantified by fractional anisotropy (FA) which reflects the coherence of directional diffusion of water in tissues, and the apparent diffusion coefficient (ADC) which measures the magnitude of diffusion. Studies in ALS have generally found reduced FA (1–10) and increased ADC (4–7,9) along the corticospinal tract (CST). Most studies have focused on the posterior limb of the internal capsule (1–5,8–10), whereas other regions such as the precentral gyrus (1,9,10) have not been evaluated as extensively. MRS permits the measurement of cerebral metabolites in vivo. MRS studies have consistently shown that the neuronal marker N-acetylaspartate (NAA) is diminished in ALS in areas of the brain relevant to motor function, including the precentral gyus (1–3,11–24), posterior limb of the internal capsule (1,13,16), and brainstem (11,25).

Previous studies combining DTI and MRS examined isolated components of the CST (1–3). A better understanding of the prominent motor impairment of ALS could be gained by measuring

Correspondence: S. Kalra, 2E3.18 Walter C. Mackenzie Health Sciences Centre, 8440-112 Street, Edmonton, Alberta, Canada T6G 2B7. Fax: 780 407 1325. E-mail: sanjay.kalra@ualberta.ca

(Received 18 November 2008; accepted 16 January 2009)

ISSN 1748-2968 print/ISSN 1471-180X online
DOI: 10.3109/17482960902756473

diffusional and metabolic changes throughout the entire course of the CST, as is the objective of this study. With this aim, we extended our previous DTI analysis from the level of the corona radiata to the cerebral peduncle (7) to include the precentral gyrus and, additionally, we incorporated a multivoxel magnetic resonance spectroscopic imaging (MRSI) protocol to evaluate metabolic changes from the motor cortex to the midbrain. Previous studies have used single voxel or axial multivoxel MRS techniques; however, these have limitations in the ability and efficiency to study the intracranial portion of the CST. Thus, we developed a coronal multivoxel MRSI protocol that would permit its contiguous evaluation.

Materials and methods

Subjects and clinical evaluation

Patients with a clinical diagnosis of probable or definite ALS according to the El Escorial (26) criteria (having both UMN and LMN signs) were recruited. The DTI findings (between the corona radiata and the cerebral peduncle) on the majority of these subjects have been reported previously (7). The study was approved by the Human Research Ethics Board and subjects gave informed consent. General disability was assessed using the ALS Functional Rating Scale (ALSFRS) (27). Measures of UMN function included the modified Ashworth spasticity scale, and finger and foot tapping rate (28). The rate of disease progression was estimated as follows: rate = (40-ALSFRS)/symptom duration (4). Healthy control subjects were free of neurological or psychiatric disease.

Image acquistion

Imaging was performed on a 1.5 tesla MR system (Magnetom Sonata, Siemens Medical Systems). Sagittal (TR = 6860 ms, TE = 112 ms) and transverse (TR = 6950 ms, TE = 113 ms) T2W images were acquired. Coronal T2W (TR = 7480 ms, TE = 113 ms) and 3D MPRAGE (TR = 1890 ms, TE = 4.38 ms, TI = 1100 ms, voxel size $1 \times 1 \times 1$ mm) imaging followed with an angulation parallel to the CST as viewed on sagittal images. Angulation was further refined by ensuring a coronal slice intersected the cerebral peduncles and the hyperintense signal of the CST in the posterior limb of the internal capsule and corona radiata on axial images.

A 2D spin-echo MRSI sequence was used (TR = 1500 ms, TE = 135 ms, $n = 4$, 12×12 phase encodes interpolated to a 16×16 matrix, FOV 160×160 mm, voxel size $1 \times 1 \times 1.5$ cm) with the slab angulated to the plane of the coronal images and positioned to enclose the CST (Figure 1A).

Coronal DT images were acquired using spin-echo echo planar imaging (20 contiguous slices (no gap), slice thickness = 5 mm, TR = 3200 ms, TE = 88 ms, matrix size = 128×128 zero-filled to 256×256, 75% phase partial Fourier, FOV = 220×220 mm, 6 diffusion gradient directions, b = 1000 s/mm^2, 8 averages). A non-diffusion weighted image (b = 0 s/mm^2) was also acquired.

MR data processing

The MPRAGE images were coregistered to the non-diffusion weighted (b = 0) reference image using SPM5 software (http://www.fil.ion.ucl.ac.uk/spm/software/spm5/, Friston, 2004). DTIstudio (Johns Hopkins University, Baltimore, MD) was used to derive diffusion maps for FA, trace ADC, the three eigenvalues (λ_1, λ_2, λ_3), and a colour map encoding principal diffusivity (the eigenvector associated with λ_1). Three-dimensional renderings of the cortex were created using MRIcro (v1.40, freeware, Chris Rorden) (29) from the MPRAGE datasets.

DTI analysis

Images were analysed by a single examiner (TEP) blinded to diagnosis. Given the considerable variation in the anatomy of the precentral gyrus (30), axial, coronal, and sagittal images and the three-dimensional renderings were used to confirm identification of the precentral gyrus on the coregistered DTI maps. The subcortical white matter (WM) of the entire precentral gyrus was segmented manually on multiple coronal slices of the FA maps using ImageJ (v1.37, Wayne Rasband, National Institutes of Health, USA) (Figure 2A). Grey matter is characterized by an FA between 0.1 and 0.2 (31). To minimize the possibility of partial volume contamination and to increase objectivity, a threshold FA of 0.3 was used for voxel inclusion. The CST caudal to the precentral gyrus was manually traced from the corona radiata to the cerebral peduncle and subdivided into the corona radiata, posterior limb of the internal capsule, and cerebral peduncle (Figure 2B) as previously described (7). Bilateral mean FA and ADC were measured in these sub-regions and the precentral gyrus.

Prior studies have evaluated the utility of using small discrete regions of interest (ROIs) placed in the precentral gyrus. To compare our method of segmentation of the entire precentral gyrus we also measured diffusion indices in a circular ROI (16 mm^2) placed in the WM of the precentral gyrus (Figure 2C).

MRSI analysis

Processing of the spectroscopic data and determination of peak area ratios (NAA/Cr, NAA/Cho, Cho/Cr)

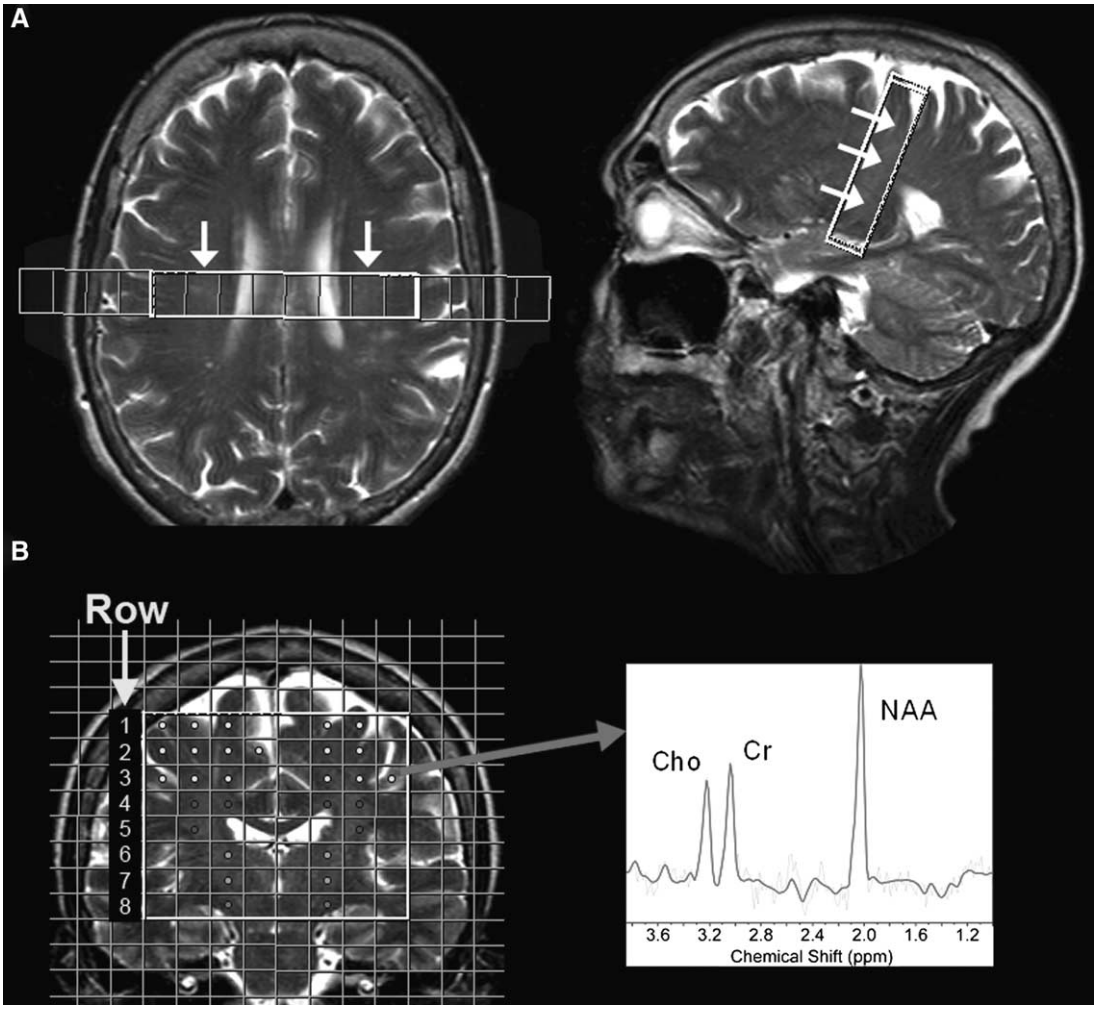

Figure 1. Magnetic resonance spectroscopic imaging. Axial, sagittal, and coronal T2-weighted MR images demonstrate placement of the volume of interest (VOI, white box). A) The hyperintense signal of the CST within the VOI is indicated by white arrows. B) Dots indicate selected voxels that include the CST. Metabolite ratios from the CST were analyzed by row to do a spatial analysis as demonstrated in Figure 3 and grouped by anatomical region (yellow dots = precentral gyrus, blue dots = corona radiata, green dots = posterior limb of the internal capsule, red dots = cerebral peduncle). At right is a sample spectrum from a single voxel; Cho = choline, Cr = creatine, NAA = N-acetylaspartate.

for each voxel was performed using LCModel (http://www.s-provencher.com/pages/lcmodel.shtml). Voxels were assigned to the precentral gyrus, corona radiata, posterior limb of the internal capsule, or cerebral peduncle (Figure 1B) if at least 50% of its contents contained the structure. Those assigned to the precentral gyrus were within the boundaries of the ROI drawn on the FA map. Metabolite ratios for each region (e.g. precentral gyrus) were calculated by determining the average ratio for all voxels assigned to that region.

Statistical analysis

Multivariate analyses of covariance (MANCOVA) were performed initially to test differences in each of bilateral FA, ADC, NAA/Cho, NAA/Cr, and Cho/Cr between the control and ALS groups with age as a covariate. There were four dependent variables representing the imaging parameter for each anatomical region (e.g. FA for each of precentral gyrus, corona radiata, posterior limb of the internal capsule, and cerebral peduncle). The use of MANCOVA reduces the chances of a type I error due to multiple comparisons since only a significant multivariate result for a parameter is followed by univariate analyses to determine the region which is abnormal. Relationships were quantified by Pearson (p) and Spearman rank (R) correlation coefficients. Correlations with clinical measures lacking lateral bias (age, symptom duration, ALSFRS, and disease rate) were tested with bilateral diffusion and spectroscopy results. Unilateral Ashworth scores and tapping speeds were tested for associations with contralateral imaging results. Statistical significance was set at a two-tailed $p < 0.05$.

Receiver operating characteristic (ROC) analysis was performed (MedCalc Software version 7.4,

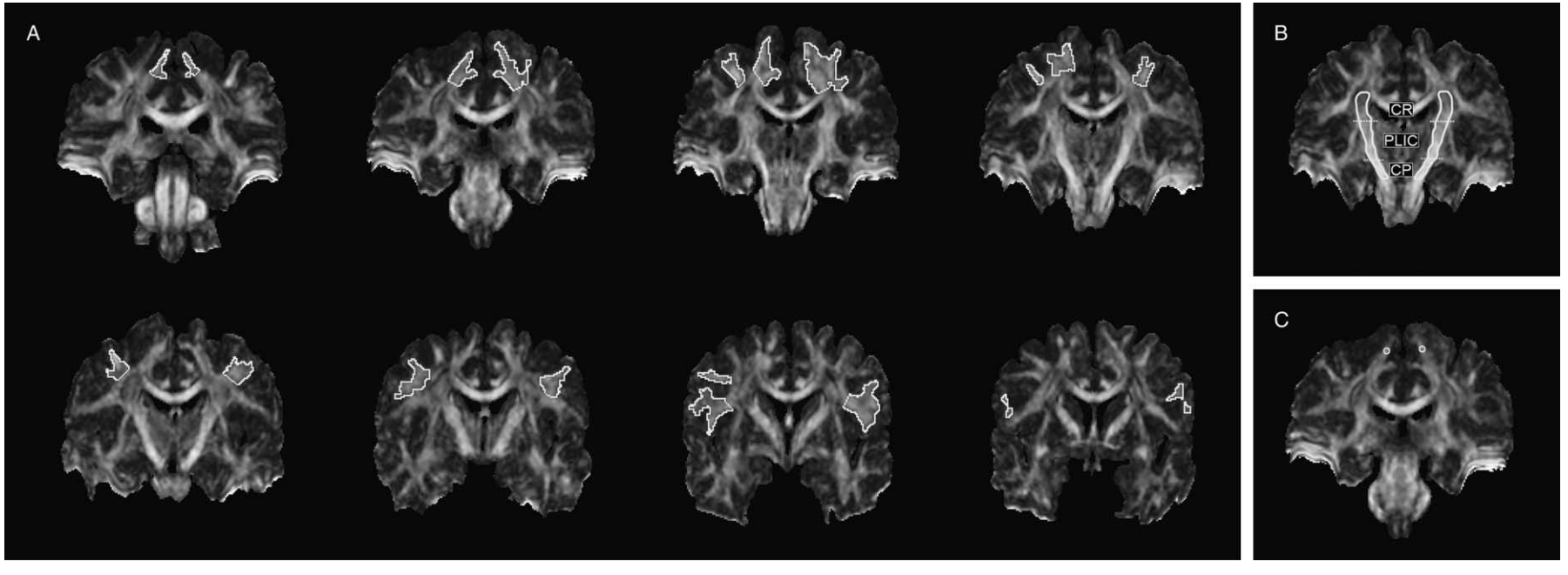

Figure 2. Diffusion tensor imaging – regional delineation of the corticospinal tract. A) The subcortical white matter of the precentral gyrus was labeled on a sequence of contiguous coronal FA maps. This sequence from a single subject proceeds anteriorly from the top left to the bottom right image. B) The CST caudal to the precentral gyrus was outlined on a single coronal FA image and was subdivided into corona radiata, posterior limb of the internal capsule, and cerebral peduncle. C) Diffusion indices were determined from a circular ROI in the precentral gyrus in both hemispheres to compare with the results of the segmentation of the entire precentral gyrus as in A).

Table I. Quantitative regional analysis of DTI and MRSI parameters in the corticospinal tract of ALS patients and healthy controls.

	Precentral gyrus		Corona radiata		Internal capsule		Cerebral peduncles	
	ALS	Controls	ALS	Controls	ALS	Controls	ALS	Controls
FA	$0.412 \pm 0.012^{\dagger}$	0.425 ± 0.014	0.487 ± 0.058	0.457 ± 0.039	0.655 ± 0.044	0.651 ± 0.027	$0.727 \pm 0.037^{\star}$	0.751 ± 0.030
ADC	0.850 ± 0.041	0.836 ± 0.042	0.803 ± 0.040	0.775 ± 0.046	0.758 ± 0.041	0.745 ± 0.043	0.740 ± 0.044	0.743 ± 0.033
NAA/Cho	$4.984 \pm 0.449^{\S}$	6.079 ± 0.685	$4.825 \pm 0.485^{\S}$	5.800 ± 0.542	5.053 ± 0.570	5.272 ± 0.502	4.871 ± 1.110	5.413 ± 0.699
NAA/Cr	$1.812 \pm 0.154^{\dagger}$	1.985 ± 0.157	$2.053 \pm 0.156^{\S}$	2.327 ± 0.188	1.832 ± 0.180	1.904 ± 0.138	1.916 ± 0.334	2.066 ± 0.240
Cho/Cr	$0.366 \pm 0.027^{\ddagger}$	$0.331 \pm 0.0.040$	0.428 ± 0.034	0.405 ± 0.048	0.367 ± 0.028	0.364 ± 0.032	0.398 ± 0.028	0.387 ± 0.063

Results are reported as bilateral mean $\pm$ standard deviation. FA: fractional anisotropy; ADC: apparent diffusion coefficient ($\times 10^{-3}$ mm^2/s); NAA: N-acetylaspartate; Cho: choline; Cr: creatine. $^{\star}p<0.1$, $^{\dagger}p<0.05$, $^{\ddagger}p<0.01$, $^{\S}p<0.001$.

Mariakerke, Belgium) for imaging parameters that significantly differed between patients and controls. The sensitivity and specificity for a parameter were determined at the cut-off value with the highest accuracy (minimal false negatives and false positives) as determined by MedCalc.

Results

Fourteen patients (male:female, 6:8; age, 54 ± 15 years; limb:bulbar onset, 12:2, ALSFRS, 30 ± 6) and 14 healthy age-matched controls (male:female, 8:6; age, 53 ± 12 years) were studied. Patients were clinically diagnosed with probable ($n=11$) or definite ($n=3$) ALS (26). Patients had symptoms ranging from 10 to 43 months in duration, except one who had symptoms for 72 months.

Multivariate analyses (MANCOVA) revealed a significant group difference for FA, NAA/Cho, NAA/Cr, and Cho/Cr between ALS patients and controls. Accordingly, a univariate analysis was performed for each of these parameters to determine which of the regions of the CST were abnormal.

Diffusion tensor imaging

FA was reduced bilaterally in the WM of the precentral gyrus in ALS patients and reduced FA in the cerebral peduncles showed a trend towards significance (Table I). In contrast to FA calculated from the entire precentral gyrus, FA derived from a circular ROI placed in the left and right subcortical white matter of the precentral gyrus was not significantly reduced in patients compared to controls (0.369 ± 0.057 vs. 0.384 ± 0.051, $p=0.47$). ADC in patients was not different from controls. WM volumes were not different between patients and controls; precentral gyrus WM volume was slightly lower in ALS (11.3 ± 2.7 vs. 13.0 ± 1.8), but this did not reach statistical significance.

Magnetic resonance spectroscopic imaging

MRS data of good quality were obtained from the precentral gyrus, corona radiata, and posterior limb of the internal capsule in all but one patient and one control. In the cerebral peduncles, spectra adequate for analysis were available from five patients and eight controls (MRS of the cerebral peduncles is technically challenging due to the presence of vasculature and small volumes of tissue). The spatial metabolite plots for controls (Figure 3) show that NAA/Cr and Cho/Cr progressively increase and NAA/Cho decreases in a rostral-to-caudal direction until near the internal capsule. The plots reveal reduced NAA/Cr and NAA/Cho throughout the CST in patients, which is statistically significant in the precentral gyrus and corona radiata (Figure 3,

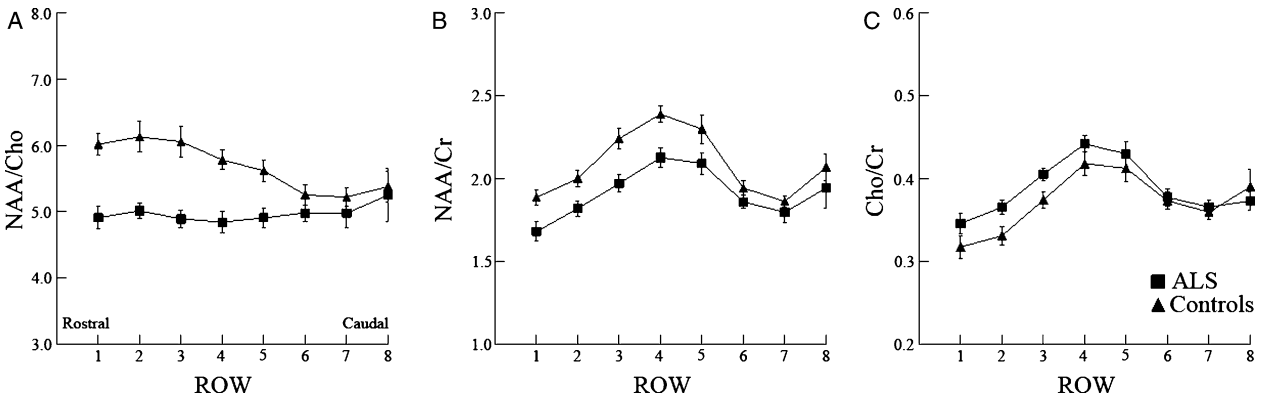

Figure 3. Spatial variation of metabolite ratios along the corticospinal tract (left to right represents rostral to caudal – see Figure 1). NAA/Cho and NAA/Cr are reduced throughout the CST with statistically significant abnormalities present more rostrally (see also Table 1). Cho/Cr is increased in the rostral portion of the CST. Error bars represent standard error.

Table I). No significant changes in any of the metabolite ratios were found in the posterior limb of the internal capsule or cerebral peduncles. The pattern for each of NAA/Cr and Cho/Cr across the CST is similar between controls and patients, suggesting that the observed spatial variation is dependent largely on Cr levels along the tract. While NAA/Cho in controls declines rostro-caudally along the CST, in patients this pattern is not found as NAA/Cho is reduced rostrally and remains low throughout the CST. NAA/Cho was used for subsequent correlative analyses given its greater magnitude of change compared to the other metabolite ratios.

Receiver operating characteristic analysis

Sensitivity and specificity were calculated using ROC curves for imaging parameters that were significantly different in patients compared to controls in the precentral gyrus. This included FA (sensitivity = 79%, specificity = 79%, cut-off = 0.422), NAA/Cho (sensitivity = 100%, specificity = 85%, cut-off = 5.640), NAA/Cr (sensitivity = 54%, specificity = 100%, cut-off = 1.799), and Cho/Cr (sensitivity = 69%, specificity = 85%, cut-off = 0.354).

Analysis of relationships

In the precentral gyrus of ALS patients, lower NAA/Cho correlated with shorter symptom duration ($r = 0.66$, $p = 0.02$) and a faster disease progression rate ($r = -0.65$, $p = 0.008$) (Figure 4). A similar association of NAA/Cho with progression rate was present in the corona radiata ($r = -0.65$, $p = 0.02$). Greater spasticity correlated with a higher ADC ($R = 0.52$, $p = 0.005$) in the contralateral precentral gyrus, with a statistical trend observed with lower FA ($R = -0.39$, $p = 0.06$). Statistical trends were also present for slower tapping speeds to be associated with lower FA ($r = 0.35$, $p = 0.08$) and higher ADC ($r = -0.36$, $p = 0.07$) in the contralateral precentral gyrus. Neither DTI nor MRSI indices correlated with ALSFRS scores. NAA/Cho did not correlate with FA or ADC in any region.

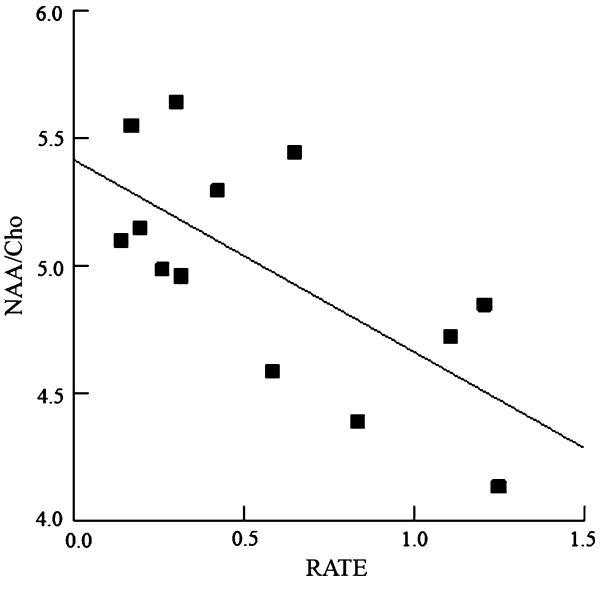

Figure 4. A faster disease progression rate was associated with lower NAA/Cho in the precentral gyrus ($r = -0.65$, $p = 0.008$).

Discussion

The objective of this study was to evaluate white matter integrity and neurochemistry in the intracranial course of the CST in patients with ALS. Two complementary imaging techniques were used to gain insight into pathogenesis and evaluate the performance of imaging parameters as surrogate markers of degeneration.

We found CST involvement in ALS detectable by DTI and MRSI to be focused in the precentral gyrus. The most abnormal result was an 18% reduction in NAA/Cho, whereas the decrease in FA was quite small (3%). Given that NAA/Cho had a better sensitivity-specificity profile and was considerably more accurate at discriminating patients from controls among these specific subjects, it may be a preferred surrogate marker of degeneration in ALS. It may also be the preferred spectroscopic marker over NAA/Cr since the latter revealed a spatial distribution along the CST similar to Cho/Cr, suggesting that the distribution was significantly dependent on Cr levels. Further studies are required with more subjects and with non-ALS disease groups to refine the potential of these imaging parameters as diagnostic and surrogate markers.

Decreased NAA/Cho can reflect neuronal loss/dysfunction (decreased NAA) or membrane turnover/gliosis (increased Cho), whereas reduced FA suggests frank axonal loss or myelin degradation. Thus, the greater abnormalities in MRSI could be a reflection of a population of neurons that are dysfunctional, perhaps in a stage preceding frank structural change that is then detected by DTI. The discrepancy in magnitude of change in spectroscopic and diffusion parameters has been reported previously, including a recent large study that combined MRSI of the motor cortex and DTI of the posterior limb of the internal capsule in 64 patients (3).

The small magnitude of change in FA can also partly be explained by the fact that FA is normally low in the precentral gyrus and corona radiata due to dispersion of CST fibres and their intermingling with U-fibres and fibres of the association tracts that run obliquely to the CST fibres. FA increases moving caudally down the CST as the axons converge and attain a predominant rostro-caudal arrangement (7). Thus, changes in axonal integrity in

the precentral gyrus or corona radiata would not have as great an impact on FA as they would in the posterior limb of the internal capsule or cerebral peduncles where FA is much higher. We previously reported reduced FA in the cerebral peduncles (7); in this study it was reduced to a lesser degree and reached a trend to statistical significance. This discrepancy is probably due to differences in subject characteristics.

NAA/Cho correlated with measures of disease progression. The finding of lower NAA/Cho in those with shorter symptom duration and a faster progression rate suggests that reduced NAA/Cho is associated with a more aggressive phenotype. This notion is supported by a study demonstrating reduced survival in patients with decreased NAA/Cho (23). One other study has reported a similar relationship between metabolite ratios and symptom duration (2) whereas others have not (15,17, 22,24,25). The inconsistency may be due to varying progression rates and high variability in metabolite ratios found in those imaged with a short duration of symptoms. Future MRS studies in ALS should attempt to confirm the relationship between spectroscopic change and rate of disease progression.

DTI indices in the precentral gyrus correlated with clinical measures of UMN function whereas NAA/Cho did not. Thus, initial stages of neuronal dysfunction may be less apt to contribute to clinically evident motor impairment but may be detected by reduced NAA/Cho. Previous studies have inconsistently shown correlations of imaging parameters with clinical UMN measures (2–4,6–8,13,16,22, 24,32). Other studies using both MRS and DTI have found that clinical indicators of UMN function correlate with spectroscopic (2,3) but not diffusional (2) changes. However, these studies examined only the posterior limb of the internal capsule in their DTI analysis (2,3). The disparate results between studies are probably related to variability in clinical status of study subjects, the clinical UMN scales used, and in technical methodology.

The topographical pattern of the imaging observations sheds light on the pathogenesis of ALS. Confinement of the MRSI and DTI abnormalities to the precentral gyrus and corona radiata suggests a mechanism whereby neurodegeneration is prominent in and perhaps begins in the cortex. With the minimal changes in more caudal segments, the abnormalities in the precentral gyrus and corona radiata could reflect the involvement of interneurons and association fibres that do not contribute to the CST. Degeneration of cortical interneurons in ALS is supported by immunohistochemical (33), electrophysiological (34), and positron emission tomography (35) studies. The decrease of FA in the cerebral peduncles probably reflects degenerating CST fibres and would support a dying-back process as has been proposed for ALS (5).

Three previous studies have coupled diffusion and spectroscopic imaging (1–3); all used an ROI of a fixed dimension in the CST. In contrast, we drew an ROI to encompass all white matter of the precentral gyrus and descending CST. All studies employed a multivoxel MRSI protocol (1–3). One employed 3D MRSI (1) and the others used axial 2D MRSI (2,3); however, the former did not analyse the precentral gyrus due to technical limitations. Our 2D MRSI protocol used a coronal orientation for the specific purpose of allowing analysis of the CST from the cortex to the cerebral peduncles. Of the three prior studies, only one attempted to examine metabolite and diffusional changes along the entire intracranial CST as we did (less the precentral gyrus) (1). However, no study has evaluated relationships between diffusion and metabolic measures in each region of the CST. We did not find an association between MRSI and DTI measures. Taken together with the disparate associations found between the two imaging modalities and clinical parameters, this suggests that these two imaging techniques measure different pathological states and mechanisms leading to disability.

By placing a small circular ROI of a pre-defined size in the precentral gyrus, as many studies have previously done, we could not detect DTI changes. Thus, our method of using an ROI to include the entire subcortical WM of the precentral gyrus was superior. Inclusion of the entire precentral gyrus was not possible, however, on the single MRSI slab. Its careful positioning along the CST did permit inclusion of the majority of the CST caudal to the precentral gyrus. Spectroscopic analysis of the entire precentral gyrus would require an alternative technique, such as multislice MRSI. Our MR protocol was developed to allow acquisition of the necessary anatomic imaging, diffusion, and spectroscopic data within an acceptable time frame for human study. For this same reason, metabolite ratios were measured rather than absolute concentrations which require additional spectroscopy measurements and are also associated with greater experimental error. Cortical regions that contribute (although in lesser proportion) fibres to the CST in addition to the precentral gyrus, such as the postcentral gyrus and premotor areas, were not analysed (36). However, our protocol was focused on the precentral gyrus where the brunt of the cortical pathology is (37). In contrast to MRS, whole brain DTI analysis of the brain is possible using the method of voxel based morphometry. Such studies have been consistent with ours in demonstrating diffusional changes in the CST and, additionally, have reinforced the notion that ALS is a multisystem disorder by demonstrating involvement of areas beyond the CST and motor cortex (9,38–41). Within these studies there is

considerable variation in the spatial distribution of diffusion changes along the CST.

A limitation of this study was the incomplete MRSI data at the level of the cerebral peduncles due to the technically challenging nature of spectroscopy in this region. Absolute quantitation of spectroscopic data may allow a better understanding of the changes in individual metabolites; however, this would have considerably increased scanning time and made it impossible to collect all of the imaging data within an acceptable time frame for human study. The limitation on scanning time was the reason for the use of relatively thick (5 mm) DTI images. This thickness would be inclusive of as much of the CST within a single image plane caudal to the precentral gyrus; however, it could have resulted in partial volume averaging of non-CST tissue. Although our study detected quite robust metabolite changes, the small sample size may have hindered a full characterization of statistical relationships. A correction for multiple comparisons was not applied as the multivariate technique of MANCOVA provides some protection in this regard (42). A correction could be applied according to the number of univariate tests performed for those multivariate tests that were significant (four multivariate tests, 16 comparisons); for example, if the very conservative Bonferroni method was used then the p-value required for significance would be $p = 0.05/16$ comparisons $= 0.003$. Even with this stringent correction the major findings of this study hold, namely marked metabolic abnormalities in the motor cortex and rostral CST.

In conclusion, combined structural and metabolic imaging of the intracranial CST revealed abnormalities focused in the motor cortex. Future studies using a combination of MRSI and DTI in early stages of the disease could be instructive to elucidate the temporal and spatial pattern of CST degeneration in ALS and, in particular, to address the question of whether metabolic abnormalities precede structural changes.

Acknowledgements

Funding was provided by the University of Alberta Hospital Foundation and the MSI Foundation of Alberta. Tim Pyra received stipend support from the Alberta Heritage Foundation for Medical Research (AHFMR) and the Canadian Institutes of Health Research. Christian Beaulieu received salary support from AHFMR and Luis Concha from Promep. The authors thank Wayne Martin for helpful comments in preparing the manuscript.

Declaration of interest: The authors report no conflicts of interest. The authors alone are responsible for the content and writing of the paper.

References

1. Yin H, Lim CC, Ma L, Gao Y, Cai Y, Li D, et al. Combined MR spectroscopic imaging and diffusion tensor MRI visualizes corticospinal tract degeneration in amyotrophic lateral sclerosis. J Neurol. 2004;251:1249–54.
2. Wang S, Poptani H, Woo JH, Desiderio LM, Elman LB, McCluskey LF, et al. Amyotrophic lateral sclerosis: diffusion-tensor and chemical shift MR imaging at 3.0 T. Radiology. 2006;239:831–8.
3. Mitsumoto H, Ulug AM, Pullman SL, Gooch CL, Chan S, Tang MX, et al. Quantitative objective markers for upper and lower motor neuron dysfunction in ALS. Neurology. 2007;68:1402–10.
4. Ellis CM, Simmons A, Jones DK, Bland J, Dawson JM, Horsfield MA, et al. Diffusion tensor MRI assesses corticospinal tract damage in ALS. Neurology. 1999;53:1051–8.
5. Karlsborg M, Rosenbaum S, Wiegell M, Simonsen H, Larsson H, Werdelin L, et al. Corticospinal tract degeneration and possible pathogenesis in ALS evaluated by MR diffusion tensor imaging. Amyotroph Lateral Scler Other Motor Neuron Disord. 2004;5:136–40.
6. Hong YH, Lee KW, Sung JJ, Chang KH, Song IC. Diffusion tensor MRI as a diagnostic tool of upper motor neuron involvement in amyotrophic lateral sclerosis. J Neurol Sci. 2004;227:73–8.
7. Wong JC, Concha L, Beaulieu C, Johnston W, Allen PS, Kalra S. Spatial profiling of the corticospinal tract in amyotrophic lateral sclerosis using diffusion tensor imaging. J Neuroimaging. 2007;17:234–40.
8. Iwata NK, Aoki S, Okabe S, Arai N, Terao Y, Kwak S, et al. Evaluation of corticospinal tracts in ALS with diffusion tensor MRI and brainstem stimulation. Neurology. 2008;70:528–32.
9. Thivard L, Pradat PF, Lehericy S, Lacomblez L, Dormont D, Chiras J, et al. Diffusion tensor imaging and voxel based morphometry study in amyotrophic lateral sclerosis: relationships with motor disability. J Neurol Neurosurg Psychiatry. 2007;78:889–92.
10. Ciccarelli O, Behrens TE, Johansen-Berg H, Talbot K, Orrell RW, Howard RS, et al. Investigation of white matter pathology in ALS and PLS using tract-based spatial statistics. Hum Brain Mapp. 2008.
11. Pioro EP, Antel JP, Cashman NR, Arnold DL. Detection of cortical neuron loss in motor neuron disease by proton magnetic resonance spectroscopic imaging in vivo. Neurology. 1994;44:1933–8.
12. Gredal O, Rosenbaum S, Topp S, Karlsborg M, Strange P, Werdelin L. Quantification of brain metabolites in amyotrophic lateral sclerosis by localized proton magnetic resonance spectroscopy. Neurology. 1997;48:878–81.
13. Rooney WD, Miller RG, Gelinas D, Schuff N, Maudsley AA, Weiner MW. Decreased N-acetylaspartate in motor cortex and corticospinal tract in ALS. Neurology. 1998;50:1800–5.
14. Kalra S, Cashman NR, Genge A, Arnold DL. Recovery of N-acetylaspartate in corticomotor neurons of patients with ALS after riluzole therapy. Neuroreport. 1998;9:1757–61.
15. Block W, Karitzky J, Traber F, Pohl C, Keller E, Mundegar RR, et al. Proton magnetic resonance spectroscopy of the primary motor cortex in patients with motor neuron disease: subgroup analysis and follow-up measurements. Arch Neurol. 1998;55:931–6.
16. Schuff N, Rooney WD, Miller R, Gelinas DF, Amend DL, Maudsley AA, et al. Reanalysis of multislice (1)H MRSI in amyotrophic lateral sclerosis. Magn Reson Med. 2001;45:513–6.
17. Sarchielli P, Pelliccioli GP, Tarducci R, Chiarini P, Presciutti O, Gobbi G, et al. Magnetic resonance imaging and 1H-magnetic resonance spectroscopy in amyotrophic lateral sclerosis. Neuroradiology. 2001;43:189–97.

18. Abe K, Takanashi M, Watanabe Y, Tanaka H, Fujita N, Hirabuki N, et al. Decrease in N-acetylaspartate/creatine ratio in the motor area and the frontal lobe in amyotrophic lateral sclerosis. Neuroradiology. 2001;43:537–41.
19. Suhy J, Miller RG, Rule R, Schuff N, Licht J, Dronsky V, et al. Early detection and longitudinal changes in amyotrophic lateral sclerosis by (1)H MRSI. Neurology. 2002; 58:773–9.
20. Rule RR, Suhy J, Schuff N, Gelinas DF, Miller RG, Weiner MW. Reduced NAA in motor and non-motor brain regions in amyotrophic lateral sclerosis: a cross-sectional and longitudinal study. Amyotroph Lateral Scler Other Motor Neuron Disord. 2004;5:141–9.
21. Kaufmann P, Pullman SL, Shungu DC, Chan S, Hays AP, Del Bene ML, et al. Objective tests for upper motor neuron involvement in amyotrophic lateral sclerosis (ALS). Neurology. 2004;62:1753–7.
22. Kalra S, Hanstock CC, Martin WR, Allen PS, Johnston WS. Detection of cerebral degeneration in amyotrophic lateral sclerosis using high-field magnetic resonance spectroscopy. Arch Neurol. 2006;63:1144–8.
23. Kalra S, Vitale A, Cashman NR, Genge A, Arnold DL. Cerebral degeneration predicts survival in amyotrophic lateral sclerosis. J Neurol Neurosurg Psychiatry. 2006;77: 1253–5.
24. Kalra S, Tai P, Genge A, Arnold DL. Rapid improvement in cortical neuronal integrity in amyotrophic lateral sclerosis detected by proton magnetic resonance spectroscopic imaging. J Neurol. 2006;253:1060–3.
25. Cwik VA, Hanstock CC, Allen PS, Martin WR. Estimation of brainstem neuronal loss in amyotrophic lateral sclerosis with in vivo proton magnetic resonance spectroscopy. Neurology. 1998;50:72–7.
26. Brooks BR, Miller RG, Swash M, Munsat TL. El Escorial revisited: revised criteria for the diagnosis of amyotrophic lateral sclerosis. Amyotroph Lateral Scler Other Motor Neuron Disord. 2000;1:293–9.
27. Cedarbaum JM, Stambler N. Performance of the Amyotrophic Lateral Sclerosis Functional Rating Scale (ALSFRS) in multicentre clinical trials. J Neurol Sci. 1997;152 (Suppl 1):S1–9.
28. Kent-Braun JA, Walker CH, Weiner MW, Miller RG. Functional significance of upper and lower motor neuron impairment in amyotrophic lateral sclerosis. Muscle & Nerve. 1998;21:762–8.
29. Smith SM. Fast robust automated brain extraction. Hum Brain Mapp. 2002;17:143–55.
30. Rademacher J, Burgel U, Geyer S, Schormann T, Schleicher A, Freund HJ, et al. Variability and asymmetry in the human precentral motor system. A cytoarchitectonic and myeloarchitectonic brain mapping study. Brain. 2001;124:2232–58.
31. Mori S, van Zijl PC. Fibre tracking: principles and strategies – a technical review. NMR Biomed. 2002;15:468–80.
32. Ellis CM, Simmons A, Andrews C, Dawson JM, Williams SC, Leigh PN. A proton magnetic resonance spectroscopic study in ALS: correlation with clinical findings. Neurology. 1998;51:1104–9.
33. Maekawa S, al Sarraj S, Kibble M, Landau S, Parnavelas J, Cotter D, et al. Cortical selective vulnerability in motor neuron disease: a morphometric study. Brain. 2004;127: 1237–51.
34. Ziemann U, Winter M, Reimers CD, Reimers K, Tergau F, Paulus W. Impaired motor cortex inhibition in patients with amyotrophic lateral sclerosis. Evidence from paired transcranial magnetic stimulation. Neurology. 1997;49:1292–8.
35. Lloyd CM, Richardson MP, Brooks DJ, Al Chalabi A, Leigh PN. Extramotor involvement in ALS: PET studies with the GABA(A) ligand [(11)C]flumazenil. Brain. 2000;123:2289–96.
36. Parent A. Carpenter's Human Neuroanatomy. 9th edn. Baltimore: Williams and Wilkins; 1996.
37. Martin JE, Swash M. The pathology of motor neuron disease. In: Leigh PN, Swash M, editors. Motor Neuron Disease. Biology and Management. London: Springer-Verlag; 1995. pp 93–118.
38. Abe O, Yamada H, Masutani Y, Aoki S, Kunimatsu A, Yamasue H, et al. Amyotrophic lateral sclerosis: diffusion tensor tractography and voxel-based analysis. NMR Biomed. 2004;17:411–6.
39. Sach M, Winkler G, Glauche V, Liepert J, Heimbach B, Koch MA, et al. Diffusion tensor MRI of early upper motor neuron involvement in amyotrophic lateral sclerosis. Brain. 2004;127:340–50.
40. Sage CA, Peeters RR, Gorner A, Robberecht W, Sunaert S. Quantitative diffusion tensor imaging in amyotrophic lateral sclerosis. Neuroimage. 2007;34:486–99.
41. Agosta F, Pagani E, Rocca MA, Caputo D, Perini M, Salvi F, et al. Voxel based morphometry study of brain volumetry and diffusivity in amyotrophic lateral sclerosis patients with mild disability. Hum Brain Mapp. 2007;28:1430–8.
42. Katz MH. Multivariable analysis: a practical guide for clinicians. Cambridge: Cambridge University Press, 1999.